



## Original article

The anti-hepatitis B virus and anti-hepatotoxic efficacies of solanopubamine, a rare alkaloid from *Solanum schimperianum*

Mohammad K. Parvez\*, Mohammed S. Al-Dosari, Md. Tabish Rehman, Adnan J. Al-Rehaily, Ali S. Alqahtani, Mohammad F. Alajmi

Department of Pharmacognosy, College of Pharmacy, King Saud University, Riyadh, Saudi Arabia

## ARTICLE INFO

## Article history:

Received 10 November 2021

Accepted 2 February 2022

Available online 7 February 2022

## Keywords:

*Solanum schimperianum*

Solanopubamine

Hepatitis B virus

Anti-HBV alkaloids

Hepatoprotection

Caspase

## ABSTRACT

Chronic liver disease caused by hepatitis B virus (HBV) remains an important health issue. Though there are effective HBV-polymerase inhibitors (e.g., lamivudine), their prolonged use leads to emergence of drug-resistant (polymerase mutant) strains. Several herbal formulations and phytochemicals have been therefore, reported as potential anti-HBV agents with no sign of resistance in experimental and clinical settings. In this study, we assessed the anti-HBV as well as hepatoprotective salutations of solanopubamine, a rare alkaloid isolated from *S. schimperianum*. In cultured HepG2.2.15 cells, solanopubamine showed marked anti-HBV activity in a time and dose-dependent manner. Solanopubamine (30  $\mu$ M) efficiently inhibited HBsAg and HBeAg expressions by 66.5%, 70.5%, respectively as compared to 82.5% and 86.5% respective inhibition by lamivudine (2  $\mu$ M) at day 5. Molecular docking analyses of solanopubamine revealed formations of stable complexes with lamivudine-sensitive as well as lamivudine-resistant polymerase through interactions of catalytic 'YMDD/YIDD' motif residues. Moreover, solanopubamine attenuated DCFH-induced oxidative and apoptotic damage and restored HepG2 cell viability by 28.5%, and downregulated caspase-3/7 activations by 33%. Further docking analyses of solanopubamine showed formation of stable complexes with caspase-3/7. Taken together, our data demonstrates promising anti-HBV and anti-hepatotoxic therapeutic potential of solanopubamine, and warrants further molecular and pharmacological studies.

© 2022 The Author(s). Published by Elsevier B.V. on behalf of King Saud University. This is an open access article under the CC BY-NC-ND license (<http://creativecommons.org/licenses/by-nc-nd/4.0/>).

## 1. Introduction

Liver function is often compromised due to metabolic disorders, toxicological inflammation or hepatotropic viral infections. Hepatitis B virus (HBV) associated chronic liver diseases such as cirrhosis and carcinoma account for substantial morbidity and mortality, worldwide (Williams, 2006; Tang et al., 2018). Though there are effective nucleoside analogs i.e. HBV-polymerase inhibitors (lamivudine, adefovir, entecavir etc.), prolonged treatment eventually leads to emergence of drug-resistant (HBV-polymerase mutants)

starins (Devi and Locarnini, 2013). In recent times, several herbal formulations or natural flavonoids, terpenes, polyphenols, saponins, lignans, alkaloids and anthraquinones have offered great promises as potential anti-HBV drugs with no sign of resistance (Wang et al., 2012; Parvez et al., 2016, Arbab et al., 2017; Parvez et al., 2019a; Parvez et al., 2019b; Parvez et al., 2020). Therefore, identification and development of novel and efficacious natural anti-HBV agents are essentially required.

*Solanum* is one of the pharmacologically important alkaloids-rich genus of family Solanaceae with worldwide distribution, including Saudi Arabia representing sixteen species, such as *Solanum schimperianum*, *S. villosum*, *S. coagulans*, *S. glabratum*, *S. incanum*, *S. nigrum* and *S. surattense* (Chaudhary, 2001). Notably, of over 35 plant species used in Saudi traditional medicine to treat various liver diseases (Al-Asmari et al., 2014; Rahman et al., 2014), mostly still lack experimental or pre-clinical validations. In view of this, we have recently screened a library of medicinal plant extracts, including *Solanum spp.* for their *in vitro* and *in vivo* cell proliferative, anti-oxidative, anti-hepatotoxic and anti-HBV activities (Arbab et al., 2015; Arbab et al., 2016; Arbab et al.,

\* Corresponding author at: Department of Pharmacognosy, College of Pharmacy, King Saud University, Riyadh 11451, Saudi Arabia.

E-mail addresses: [mohkhalid@ksu.edu.sa](mailto:mohkhalid@ksu.edu.sa), [khalid\\_parvez@yahoo.com](mailto:khalid_parvez@yahoo.com) (M.K. Parvez).

Peer review under responsibility of King Saud University.



Production and hosting by Elsevier

2017; Parvez et al., 2018a, Parvez et al., 2018b). Of these, *S. surattense* previously reported for steroidal alkaloid saponins and glycosides (solanoside A1 and B2) (Lu et al., 2011; Nawaz et al., 2014), have shown strong anti-oxidative and hepatoprotective efficacies in liver cell culture and rat models (Parvez et al., 2019c).

Previous phytochemical studies of *S. schimperianum* have reported isolations of several bioactive compounds viz., isoquercetin, kaempferol-3-diglucoside, kaempferol-3-O-glucopyranoside, rutin, retusin, solamargine, solamarine, solanopubamide, lupeol, and  $\beta$ -sitosterol (Coune and Denoel, 1975; Kumari et al., 1986, Al-Oqail et al., 2012). While a rare steroidal alkaloid solanopubamine from *S. pubescence* has been reported (Kumari et al., 1985), solanopubamine isolated *S. schimperianum* has been shown to have non-cytotoxic and antifungal activities (Al-Rehaily et al., 2013). Notably, our high-performance thin-layer chromatography analysis of six *Solanum* spp. has confirmed presence of solanopubamine in *S. schimperianum* only (Siddiqui et al., 2017). With this information, this study investigates the *in vitro* anti-HBV and anti-hepatotoxic therapeutic potential of solanopubamine in hepatoma cell culture model, supported by virtual structure-based docking analysis.

## 2. Material and methods

### 2.1. Plant material, compound isolation and structure determination

The isolation of solanopubamine from the alkaloidal fraction of *S. schimperianum* Hochst (voucher specimen no. 14903) grown in Saudi Arabia, including its structure determination using IR, positive ESI-MS, 1D and 2D NMR has been described elsewhere (Al-Rehaily et al., 2013). Its chemical name (3 $\beta$ -amino-5 $\alpha$ , 22 $\alpha$ H, 25 $\beta$ H-solanidan-23 $\beta$ -ol), chemical formula (C<sub>27</sub>H<sub>46</sub>N<sub>2</sub>O) and molecular weight (414.361 g/mol) were determined.

### 2.2. Cell cultures and drugs

The human hepatoma cell line HepG2 and its derivative HBV-reporter cells HepG2.2.15 obtained from Dr. S. Jameel (ICGEB, Delhi Delhi, India) were maintained in DMEM GlutMax medium (Invitrogen, USA) reconstituted with 10% fetal bovine serum (Gibco, USA), 1x penicillin-streptomycin mix (HyClone Laboratories, USA) at 37 °C with 5% CO<sub>2</sub>. For all experiments, cells (0.5x10<sup>5</sup>/100  $\mu$ l/well) were grown in 96-well plates (Corning, USA) a day before treatment. Dichlorofluorescein (DCFH; Sigma, USA) was used as inducer of oxidative stress and cytotoxicity in HepG2 cells (Arbab et al., 2016; Parvez et al., 2018a, 2018b). The approved anti-HBV drug, lamivudine (LAM; Sigma, USA) was used as standard (Parvez et al., 2006).

### 2.3. Cell viability or toxicity assay of solanopubamine (SPB)

The effect of SPB on cells viability or toxicity was assessed using MTT cell proliferation assay kits (Tervigen, USA) to estimate the optimally safe doses. Briefly, SPB was first dissolved in dimethyl sulfoxide (DMSO; Sigma, USA) and then reconstituted in culture media to furnish five test concentrations or doses: 3.12, 6.25, 12.5, 25 and 50  $\mu$ g/ml (equivalent to 7.5, 15, 30, 60 and 120  $\mu$ M, respectively). HepG2 cells grown in 96-well plate were replenished with fresh media containing the different doses of SPB, including vehicle control (0.1% DMSO), and incubated up to 72 h. All samples were tested in triplicate and the experiment was repeated twice. The optical density (OD;  $\lambda$  = 570 nm) of the samples were recorded, using microplate reader (ELx800; BioTek, USA). Non-linear regression analysis was performed (Excel software 2010; Microsoft, USA)

to determine the 50% cytotoxic concentration (CC<sub>50</sub>) using the following equation:

$$\% \text{Cell survival} = \frac{[(\text{OD}_{\text{sample}} - \text{OD}_{\text{blank}}) / (\text{OD}_{\text{control}} - \text{OD}_{\text{blank}})] \times 100}$$

### 2.4. Dose and time-dependent analysis of HBV 's' antigen (HBsAg) inhibitions by SPB

HepG2.2.15 cells grown in 96-well plate were replenished with fresh media containing four selected doses (7.5, 15, 30 and 60  $\mu$ M) of SPB, including controls, and incubated up to 5 days. The supernatants of treated cells were collected on day 1, day 3 and day 5, and stored at –20 °C for further analysis. The secretion of HBsAg was analyzed in supernatants using the diagnostic ELISA kit (MonolisaHBsAg ULTRA, BioRad, USA) as per the kit's manual. The OD was recorded, and analyzed with reference to untreated control in Excel. All samples were tested in triplicate and the experiment was repeated twice.

### 2.5. Dose and time-dependent analysis of HBV 'e' antigen (HBeAg) inhibition by SPB

Further, the inhibitory effects of SPB (7.5, 15, 30 and 60  $\mu$ M) on HBeAg synthesis, a serological marker of HBV DNA replication were also assessed. The post-treatment HepG2.2.15 supernatants collected on day 1, day 3 and day 5 were analyzed for HBeAg expressions using the diagnostic ELISA kit (HBeAg/Anti-HBe Elisa Kit; DIAsource, Belgium) according to the manufacturer's manual. The OD was recorded, and analyzed with reference to untreated control in Excel. All samples were tested in triplicate and the experiment was repeated twice.

### 2.6. Assay for hepatoprotective activity of SPB

HepG2 cells grown in 96-well plate were replenished with fresh media containing DCFH (CC<sub>50</sub>: 20  $\mu$ M) plus SPB at a dose of 7.5, 15, 30 and 60  $\mu$ M, including untreated as well as DCFH only-treated control. After 24 and 48 h of incubations at 37 °C, MTT assay was performed, and data were analyzed in relations to the untreated control in Excel. All samples were tested in triplicate and the experiment was repeated twice.

### 2.7. Assay for anti-oxidative and anti-apoptotic activity of SPB

The efficacy of SNB against oxidative and apoptotic cell damages was evaluated by analyzing the cellular caspase-3/7 expressions. HepG2 cells grown in a 96-well plate were treated with DCFH (20  $\mu$ M) plus a dose of SPB (7.5, 15, 30 and 60  $\mu$ M), including controls. At 48 h post-treatment, cellular caspase expressions were estimated (Apo-ONE-cas3/7 assay kit; Promega, USA) as per the kit's manual. Briefly, 100  $\mu$ l of caspase-3/7 reagent was gently mixed to each culture and incubated up to 6 h in dark for at room temperature (RT). While the culture treated with caspase3/7 reagent alone acted as blank, reagent plus DMSO served as negative control. The OD was recorded and data were analyzed with reference to untreated control in Excel. All samples were tested in triplicate and repeated twice.

### 2.8. Microscopy

Direct visual observation of the SNB and DCFH treated cells for any morphological changes or toxicity was performed under an inverted microscope (Optica, 40x and 100x).

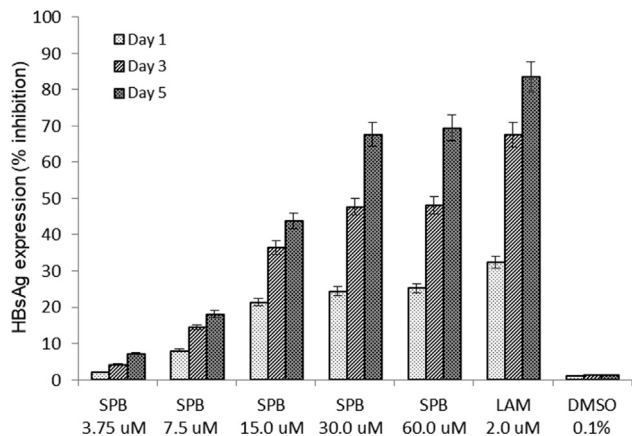


**Fig. 1.** Antiviral assay showing dose and time-dependent inhibition of HBV ‘s’ antigen (HBsAg) expressions by solanopubamine (SPB; 7.5, 15, 30 and 60 μM) relative to untreated control in HepG2.2.15 culture supernatants at day 1, 3 and 5. Lamivudine (LAM; 2 μM) served as reference drug while DMSO (0.1%) acted as vehicle control. Values on Y-axis are means of three determinations (samples in triplicate; test-repeated twice).

2.9. In silico protein modeling and ligands preparations

For the structure-based interaction analysis of SPB, the in-house modelled 3D structure of the wild type HBV-polymerase (HBV-POLwt) was used as described elsewhere (Parvez et al, 2019a). Also, using the similar computational approach, the 3D structure of LAM-resistant ‘YMDD (Tyr203-Met204-Asp-205-Asp206)’ motif mutant (YIDD; Met204Ile) of the protein (HBV-POLmut) was constructed. The SWISS-MODEL sever was employed to generate the model using HIV reverse-transcriptase protein (PDB ID: 1RTD) as a template. The overall quality of HBV-POLmut 3D model was accessed by Ramachandran plot. The 3D coordinates of caspase-3 (PDB Id: 2XYG) (Ganesan et al., 2011) and caspase-7 (PDB Id: 3IBC) (Agniswamy et al., 2009) were retrieved from PDB RCSB database (www.rcsb.org). Prior to docking analysis, any water molecules or bound hetero atoms were removed from the target proteins. Hydrogens were added and Kollman charges were assigned, and all protein structures were energy-minimized in MMFF (Merck Molecular Force Field). The 2D structures of SPB, LAM (control ligand for HBV-POL), TQ8 (control ligand for

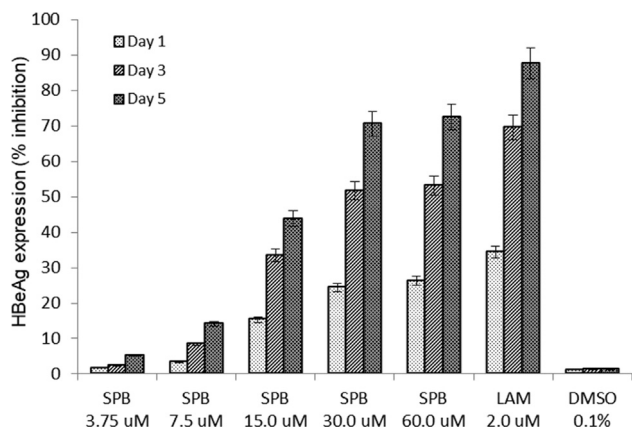


**Fig. 2.** Antiviral assay showing dose and time-dependent inhibition of HBV ‘e’ antigen (HBeAg) expressions by solanopubamine (SPB; 15, 30 and 60 μM) relative to untreated control in HepG2.2.15 culture supernatants at day 1, 3 and 5. Lamivudine (LAM; 2 μM) served as positive controls while DMSO (0.1%) acted as negative control. Values on Y-axis are means of three determinations (samples in triplicate; test-repeated twice).

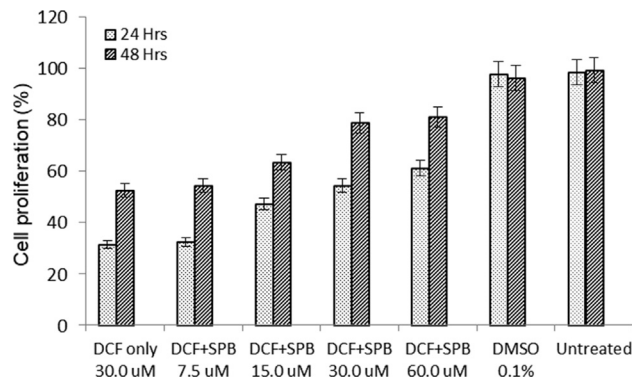


**Fig. 3.** Cell proliferative (MTT) assay showing anti-hepatotoxic activity of solanopubamine (SPB; 15, 30 and 60 μM) against dichlorofluorescin (DCF) induced oxidative stress in HepG2 cells at 24 and 48 h. DMSO (0.1%) served as vehicle control. Values on Y-axis are means of three determinations (samples in triplicate; test-repeated twice).

caspase-3), and Acetyl-YVAD-CHO (control ligand for caspase-7) were drawn in ChemDraw, following assignments of bond orders and bond angles. Further, the Gasteiger partial charges were defined and energies were minimized for all ligands in UFF (Universal Force Field) program.

2.10. Molecular docking analysis

The virtual interactions between target proteins (HBV-POLwt, HBV-POLmut, caspase-3 and caspase-7) and ligands (SPB, LAM, TQ8 and Acetyl-YVAD-CHO) were assessed by molecular docking analysis in AutoDock 4.2 (Morris et al., 2009; Al-Shabib et al., 2020). The grid boxes were defined by selecting the key amino acid residues of the published crystal structure of proteins. For HBV-POLwt and HBV-POLmut protein structures, the grid box dimensions were set to 26.3 × 26.4 × 27.5 Å, centered at 47.3 × 30.3 × 34.5 Å with 0.375 Å spacing. Similarly, the grid boxes were set to 33.3 × 28.8 × 28.3 Å centered at 36.4 × 37.4 × 31.5 Å, and 25.1 × 34.5 × 29.8 Å centered at 49.8 × -26.4 × -2.3 Å with 0.375 Å spacing for caspase-3 and caspase-7. Molecular docking was executed using LGA (Lamarck Genetic Algorithm) and Solis-Wets local search methods. For each run, 2,500,000 energy were computed and a total of 10 docking runs were executed. The analysis parameters viz., population size (150), translational step (0.2),

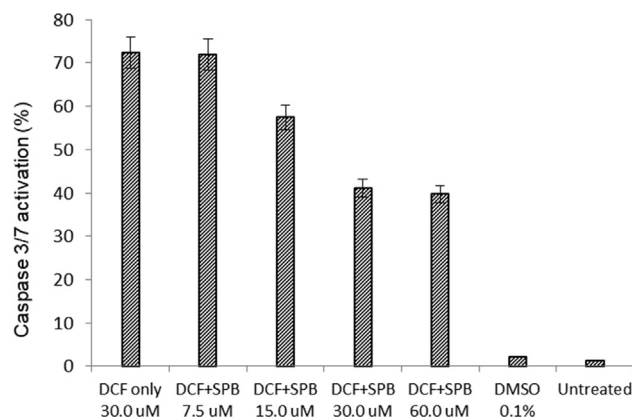


**Fig. 4.** Anti-apoptotic assay showing down regulation of cellular caspase-3/7 expression of *S. schimperi* derived solanopubamine (SPB; 15, 30 and 60 μM) in dichlorofluorescin (DCF) in HepG2 cells at 48 h. DMSO (0.1%) served as vehicle control. Values on Y-axis are means of three detrmintations (samples in triplicate; test-repeated twice).

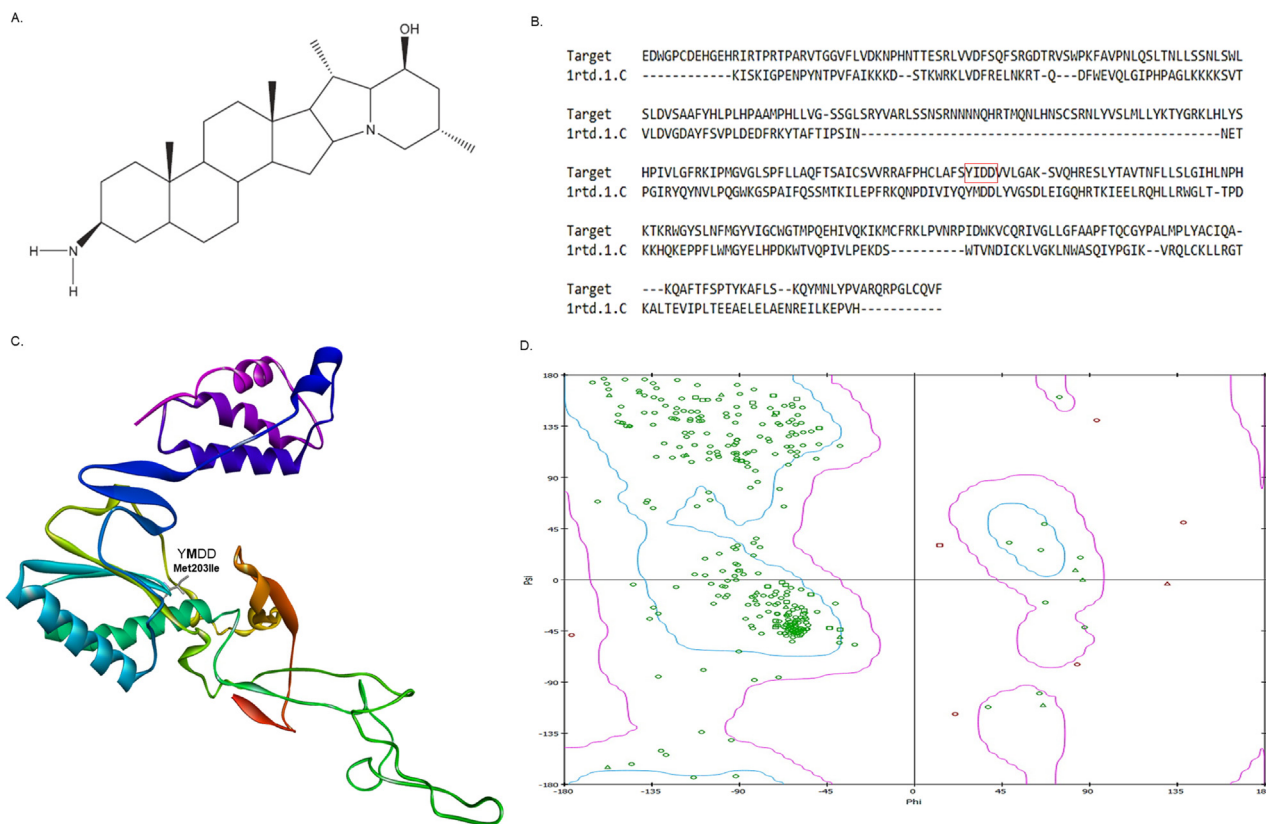


**Fig. 5.** Representations of (A) 2D structure of solanopubamine, (B) polymerase target-template sequence alignment, (C) 3D model of mutant-polymerase, and (D) validation by Ramachandran plot.

quaternions (5) and torsions (5) were set. Further, the van der Waals' and electrostatic parameters were calculated by using distance-dependent dielectric function. The docking affinity ( $K_b$ ) of each interacting ligand-protein was determined from docking energy ( $\Delta G$ ) using the following equation (Rehman et al., 2016):

$$\Delta G = -RT \ln K_b \quad (R = \text{universal gas constant, } 1.987 \text{ cal/mol/K; } T = \text{temperature, } 298 \text{ K}).$$

### 2.11. Statistical analysis

Data of all triplicated samples were expressed as mean  $\pm$  S.E.M. In a set of data, determination of total variation was performed by one-way analysis of variance (ANOVA), following the Dunnett's-test (Excel 2010; Microsoft OK, USA).  $P < 0.01$  was considered significant.

## 3. Results

### 3.1. Non-cytotoxicity of SPB

SPB tested up to 60  $\mu\text{M}$  (optimal dose) did not show any sign of cytotoxicity at 72 h. This was in accordance with the observed morphological integrity of HepG2 cells under microscope. The  $\text{CC}_{50}$  value was therefore, not determined.

### 3.2. Inhibition of viral HBsAg synthesis by SPB

SPB showed significant anti-HBV activity when treated with 15–60  $\mu\text{M}$  doses for 3–5 days (Fig. 1). On day 3 post-treatment, 15, 30 and 60  $\mu\text{M}$  doses inhibited HBsAg by about 35.5%, 46.6% and 47%. On day 5, the estimated optimal HBsAg inhibitions with 30 and 60  $\mu\text{M}$  doses were 66.5% and 68.2%, respectively as compared to

82% inhibition by LAM, the reference drug (Fig. 1). Notably, treatment with 60  $\mu\text{M}$  dose had no significant effect. Moreover, because prolong culture with higher doses of SPB resulted in cell overgrowth and death, the assay was terminated at day 5.

### 3.3. Down regulation of virus replication by SPB

SPB showed significant anti-HBV activity with 15–60  $\mu\text{M}$  treatment for 3–5 days (Fig. 2). On day 3, the 15, 30 and 60  $\mu\text{M}$  doses inhibited HBeAg production by about 33.5%, 50.6% and 52%, respectively. On day 5, the estimated optimal HBeAg inhibitions with 30 and 60  $\mu\text{M}$  doses were 70.5% and 72%, respectively as compared to 86.5% inhibition by LAM, the reference drug (Fig. 2). Notably, treatment with 60  $\mu\text{M}$  dose had no significant effect. Because prolong culture with higher doses of SPB resulted in cell overgrowth and death, the assay was terminated at day 5.

### 3.4. Hepatoprotection by SPB against chemical-induced oxidative damage

The dose and time-dependent cytoprotective effect of SPB against DCFH-induced hepatotoxicity was evaluated. While DCFH caused about 2.5% of HepG2 cell death, treatment with 30  $\mu\text{M}$  and 60  $\mu\text{M}$  dose of SPB markedly restored the cell viability to 78.5% and 81%, respectively as compared to untreated cells at 48 h (Fig. 3).

### 3.5. Anti-apoptotic potential of SPB via down regulation of cellular caspase-3/7

The dose and time-dependent anti-apoptotic effect of SPB against DCFH-induced HepG2 cell death was evaluated. Compared

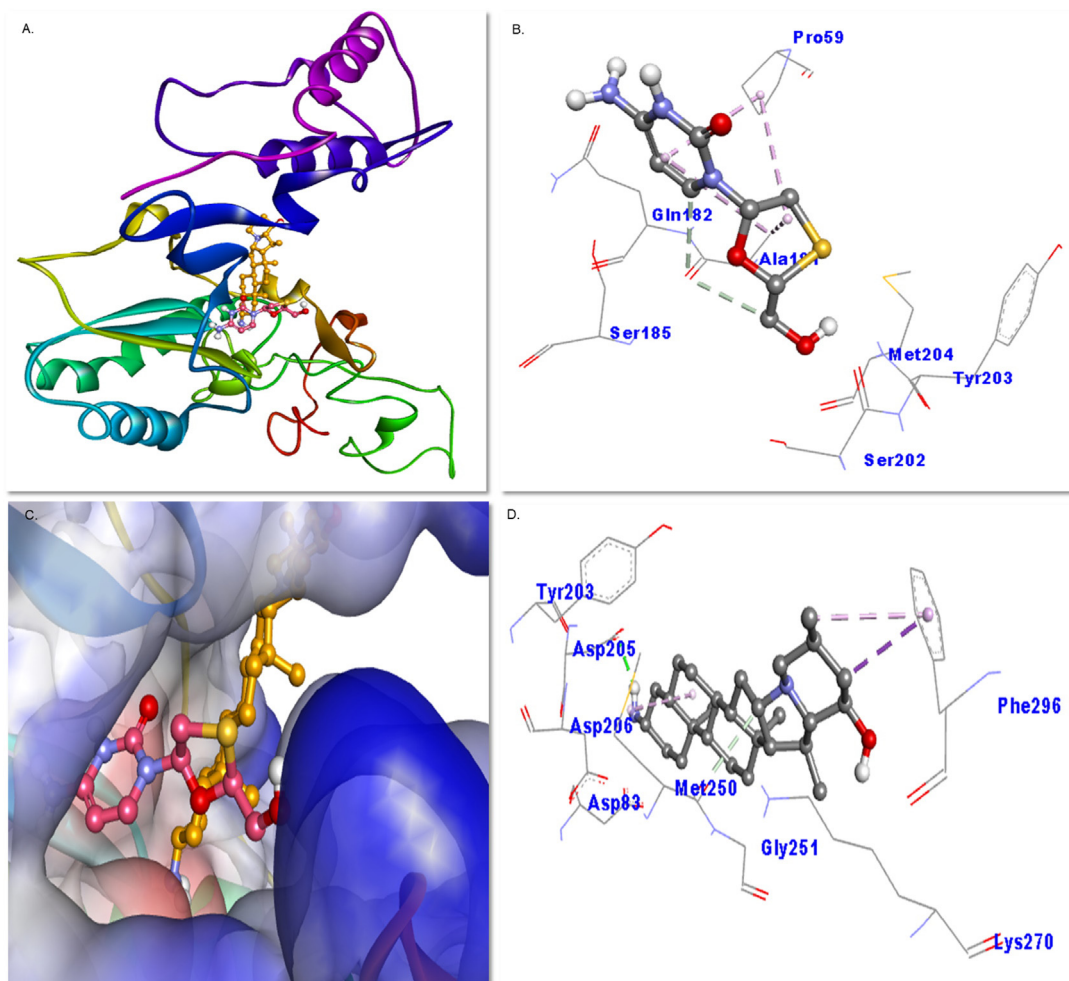


**Fig. 6.** Molecular docking analysis showing virtual interaction of wild type ('YMDD' motif) polymerase with (A and B) lamivudine, and (C and D) solanopubamine.

to DCFH-induced activation of caspase-3/7 up to 72%, treatment with 30  $\mu\text{M}$  and 60  $\mu\text{M}$  dose of SPB markedly downregulated caspase-3/7 to about 41% and 39.7%, respectively (Fig. 4).

### 3.6. Homology modeling and validation of HBV polymerase

The 2D structure of SPB drawn in ChemDraw (Fig. 5A) was used for docking analysis. The amino acid sequence of HBV-POLmut was submitted to SWISS-MODEL server to retrieve a suitable template, and searched with BLAST (Camacho et al., 2009) and HHblits (Steinegger et al., 2019) to identify evolutionary related structures. Overall 481 templates were identified, amongst which the C-chain of 1RTD (HIV-RT) was used as the template. The sequence identity, sequence similarity, and coverage score of 1RTD template were 17.56, 0.28, and 0.74 respectively. Finally, the model was built based on target-template alignment (Fig. 5B), using ProMod3 (Studer et al., 2021). The generated model (Fig. 5C) was validated by Ramachandran plot (Fig. 5D), which showed that 79.8%, 16.0%, 1.4% and 2.8% residues occupied the core or favored area, allowed region, generously allowed region, and disallowed region. The results confirmed that the overall quality of the HBV-POLmut was good and therefore used in molecular docking.

### 3.7. Interaction of SPB with HBV-POLwt

The virtual structure-based analysis showed that LAM (ligand control) and SPB were bound to the active site of HBV-POLwt

(Fig. 6A and 6B). LAM interacted with HBV-POLwt primarily through hydrophobic interaction and hydrogen bonds. It formed a hydrogen bond with Ser202:OG (3.00 Å) and two carbon hydrogen bonds with Ala181:O (3.51 Å and 3.66 Å). Also, LAM interacted with Pro59 (5.20 Å, and 4.42 Å) and Ala181 (5.12 Å, and 3.84 Å) through four hydrophobic interactions (Fig. 6C). Notably, the 'YMDD' (Tyr203-Met204-Asp-205-Asp206) motif residues Tyr203, and Met204 along with Gln182 and Ser185 further stabilized the LAM-POLwt complex by forming van der Waals' interactions. The estimated binding free energy and binding affinity of the complex were  $-5.3 \text{ kcal M}^{-1}$  and  $7.71 \times 10^3 \text{ M}^{-1}$ , respectively (Suppl. information; Table S1). SPB formed a stable complex with POLwt through hydrogen bonds as well as hydrophobic interactions (Fig. 6D). Interestingly, the 'YMDD' motif residue Asp205:OD1 formed a conventional hydrogen bond with the H-atom of SPB (2.14 Å) whereas Met250:O interacted with C-atom of SPB through a carbon-hydrogen bond (3.51 Å) (Suppl. information; Table S1). In addition, Met250, Ile269 and Phe296 interact with SPB through hydrophobic interactions. Notably, the SPB-POLwt complex was also stabilized by van der Waals' interactions involving the Tyr203 and Asp206 residues of 'YMDD' motif, including Asp83, Gly251 and Lys270. The binding energy and the binding affinity of the complex was estimated to be  $-7.5 \text{ kcal M}^{-1}$  and  $3.17 \times 10^5 \text{ M}^{-1}$ , respectively. Taken together, the POLwt residue Tyr203 was commonly involved in the interaction with both LAM and SPB.

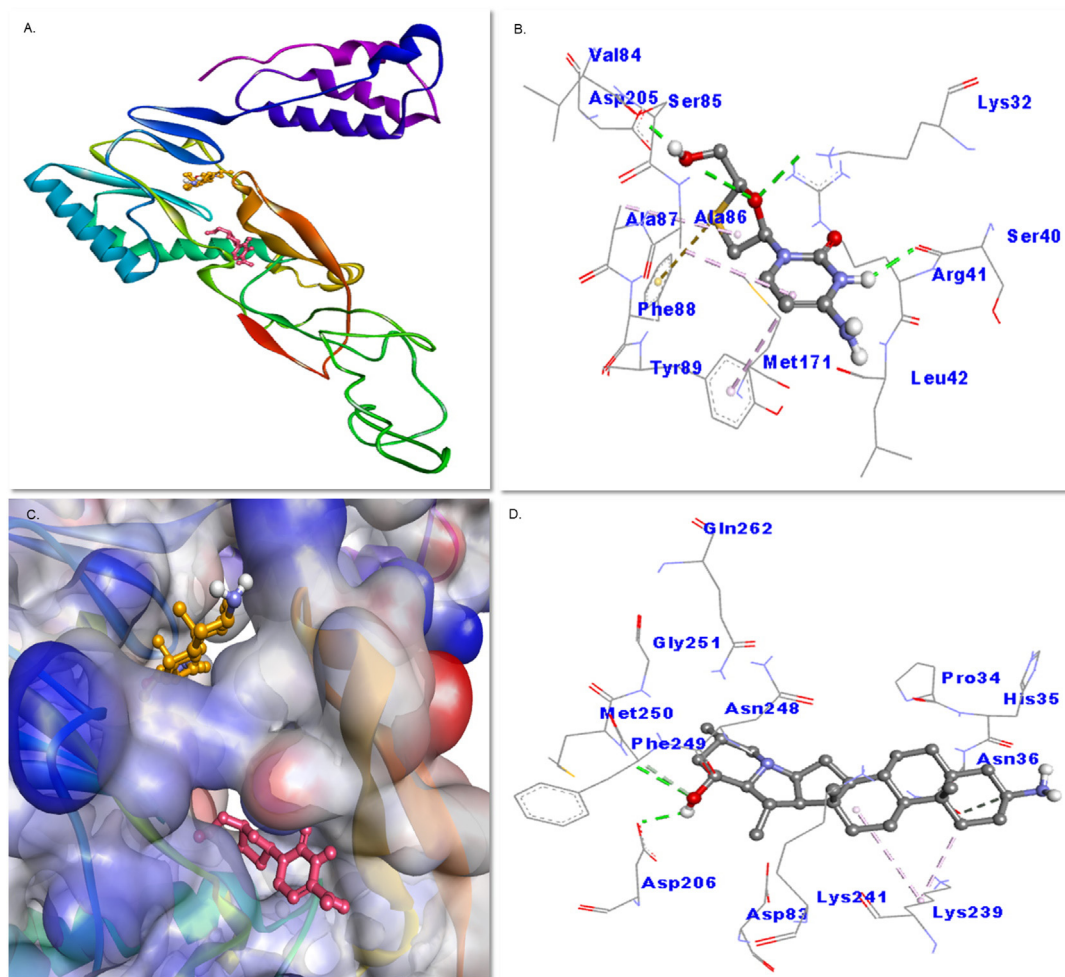


**Fig. 7.** Molecular docking analysis showing virtual interaction of mutant ('YIDD' motif) polymerase with (A and B) lamivudine, and (C and D) solanopubamine.

### 3.8. Interaction of SPB with HBV-POLmut

The docking results revealed that while SNB was bound to HBV-POLmut active site residues, LAM preferred to bind at a different site (Fig. 7A and 7B) as compared to POLwt. Lamivudine interacted with POLmut through four hydrogen bonds with LysS32:HZ1 (2.60 Å), Ser40:O (2.27 Å), Val84:O (1.91 Å) and Ala86:HN (2.94 Å). LAM also formed one Pi-S bond with Phe88 (5.45 Å), and three hydrophobic interactions with Ala86 (4.53 Å), Ala87 (5.05 Å) and Tyr89 (4.84 Å) (Fig. 7C). The complex was also stabilized by Arg41, Leu42, Ser85, Met171 and Asp205 through van der Waals' interactions. The estimated binding free energy and binding affinity was  $-5.0 \text{ kcal M}^{-1}$  and  $4.65 \times 10^3 \text{ M}^{-1}$ , respectively (Suppl. information; Table 1). The SPB and POLmut interaction was favored by conventional hydrogen bonds with the 'YMDD' motif residue Asp206:OD2 (2.19 Å) along with Met250:HN (2.92 Å). It also formed two carbon-hydrogen bonds with Asn36 (3.56 Å) and Phe249:CA (3.43 Å) (Fig. 7D). In addition, SPB also interacted with POLmut residue Lys239 (4.02 Å and 5.07 Å) through hydrophobic interactions. Moreover, the SPB-POLmut complex was also stabilized by van der Waals' interactions with Pro34, His35, Asp83, Lys241, Asn248, Gly251 and Gln262. The binding free energy and binding affinity of the complex was determined to be  $-7.2 \text{ kcal M}^{-1}$  and  $1.91 \times 10^5 \text{ M}^{-1}$ , respectively (Suppl. information; Table S1). Notably, while SPB interacted with 'YMDD' motif's active residue

Asp206 of POLmut, it also interacted with Trp203 of POLwt, and formed stable complex in both cases.

### 3.9. Interaction of SPB with Caspase-3

Molecular docking analysis showed that both TQ8 and SPB were bound to the active site residues of caspase-3 (Fig. 8A and 8B) by making three hydrogen bonds with Arg207:HN (1.88 Å), Arg207:HH11 (2.93 Å) and Arg207:HH21 (2.30 Å), and two hydrophobic interactions with Trp206 (3.75 Å, and 5.11 Å). On the other hand, residues like Ser65, Tyr204, Asn208, and Phe250 interacted through van der Waals' (Fig. 8C). The estimated docking energy and docking affinity of TQ8 and caspase-3 complex were  $-5.8 \text{ kcal M}^{-1}$  and  $1.79 \times 10^4 \text{ M}^{-1}$ , respectively (Suppl. information; Table S2). SPB formed a stable complex with caspase-3 mainly through hydrophobic interactions through its C-atom and the Arg207 O-atom (3.36 Å). In addition, SPB formed three hydrophobic interactions with Trp206 (5.27 Å) and Phe256 (5.08 Å, and 4.63 Å) of caspase-3 (Fig. 8D). The complex was also stabilized by van der Waals' interactions involving Tyr204, Asn208, Ser209, Lys210 and Phe250 residues. The binding energy and binding affinity of the complex was determined to be  $-7.4 \text{ kcal M}^{-1}$  and  $2.68 \times 10^5 \text{ M}^{-1}$ , respectively (Suppl. information; Table S2). Notably, Tyr204, Trp206, Arg207, Asn208, Ser209

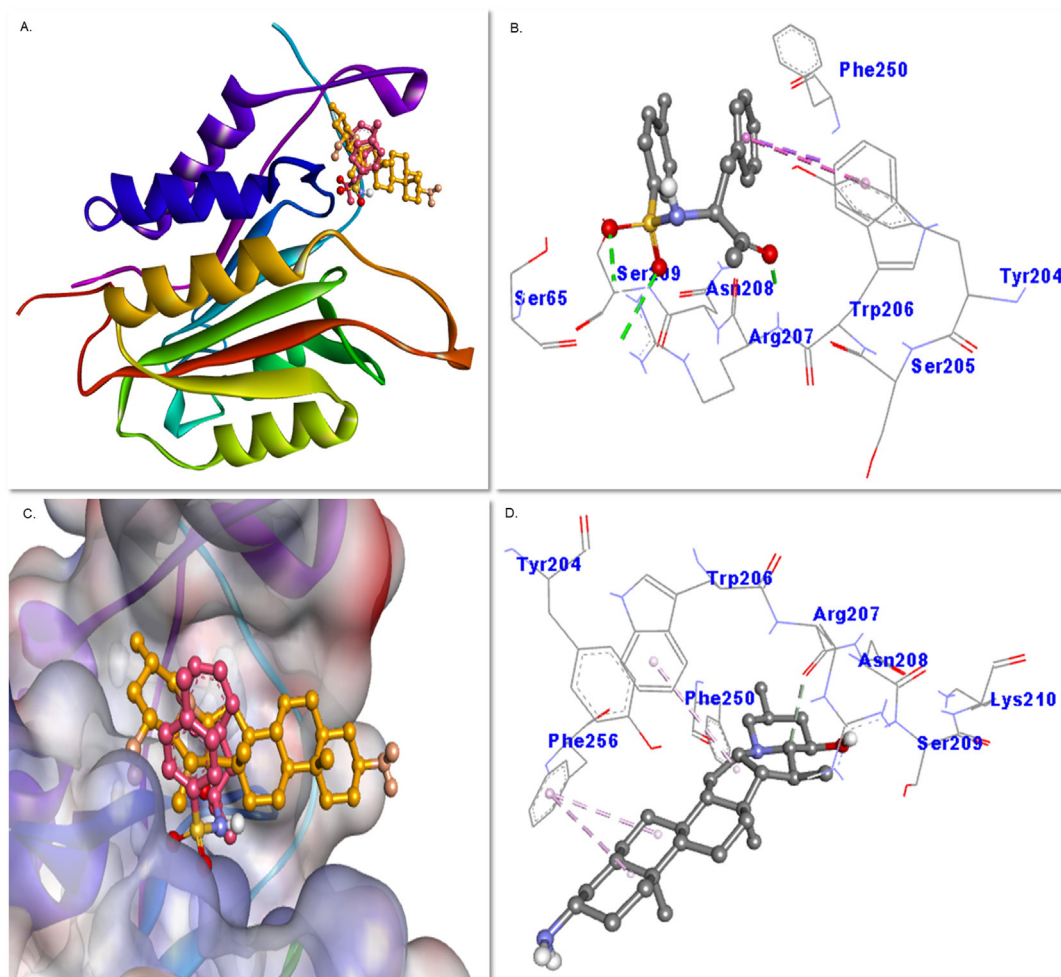


**Fig. 8.** Molecular docking analysis showing structure-based interaction of *S. schimperianum* derived solanopubamine with (A) caspase-3 and (B) TQ8, the ligand control.

and Phe250 were the most common residues of caspase-3 involved in the interaction of caspase-3 with ligand control and SPB.

### 3.10. Interaction of SPB with Caspase-7

The docking results showed that Acetyl-YVAD-CHO and SPB were bound to the active site of caspase-7 (Fig. 9A and 9B) through making six hydrogen bonds with Arg233:O (2.71 Å), Arg233:HN (2.08 Å), Arg233:HH11 (2.78 Å), Arg233:HH21 (2.54 Å), Gln276 (3.08 Å) and His272:O (2.58 Å). However, other residues such as Ser231, Trp232, Arg237, Phe273 and Phe282 established van der Waals' interactions (Fig. 9C). The calculated docking energy and docking affinity of the Acetyl-YVAD-CHO and Caspase-7 complex was  $-9.6 \text{ kcal M}^{-1}$  and  $1.10 \times 10^7 \text{ M}^{-1}$ , respectively (Suppl. information; Table 2). In the complex, SPB formed a hydrogen bond with the O-atom of His272 (2.44 Å), including two hydrophobic interactions with Trp232 (4.89 Å) and Trp240 (5.45 Å) (Fig. 9D). In addition, the van der Waals' interactions were formed by Arg233, Pro235, Arg237, Phe273, Glu274 and Gln276. The docking energy and affinity of the complex was  $-8.2 \text{ kcal M}^{-1}$  and  $1.03 \times 10^6 \text{ M}^{-1}$ , respectively (Suppl. information; Table S2). Notably, Trp232, Arg233, Pro235, Arg237, Trp240 and Glu274 were the most residues of caspase-7 which interacted with ligand control and SPB.

## 4. Discussion

Ample of bioactive plant metabolites belonging to various classes of phytochemicals have been reported for their potent *in vitro* and *in vivo* anti-HBV activities (Wang et al., 2012; Parvez et al., 2016). Nonetheless, these compounds differ in their modes of action on HBV antigens expressions and DNA replication. These activities are suggested via direct inhibition of viral products, enhancement of host-immunity or anti-inflammation as well as hepatoprotection from oxidative or apoptotic damages. We have recently demonstrated several plant extracts and bioactive phytoconstituents with promising anti-oxidative, hepatoprotective and anti-HBV activities (Arbab et al., 2017; Parvez et al., 2018a, 2018b; Parvez et al., 2019a; Parvez et al., 2019b; Parvez et al., 2020; Parvez et al., 2021). Natural alkaloids containing nitrogen in a heterocyclic ring have a range of therapeutic salutations, including anti-HBV activities *in vitro* and *in vivo*. In accordance with this, we have also reported isolation of solanopubamine, a rare steroidal alkaloid from *S. schimperianum* (Al-Rehaily et al., 2013; Siddiqui et al., 2017), which has been however, remained unexplored for its anti-HBV and hepatoprotective potential.

While HBV envelope or surface protein (HBsAg) is a serological marker of infection, the processed-product of HBV pre-Core protein (HBcAg) is a gold-marker of active HBV DNA replication (Parvez et al., 2016). Of the available HBV-reporter cell lines,

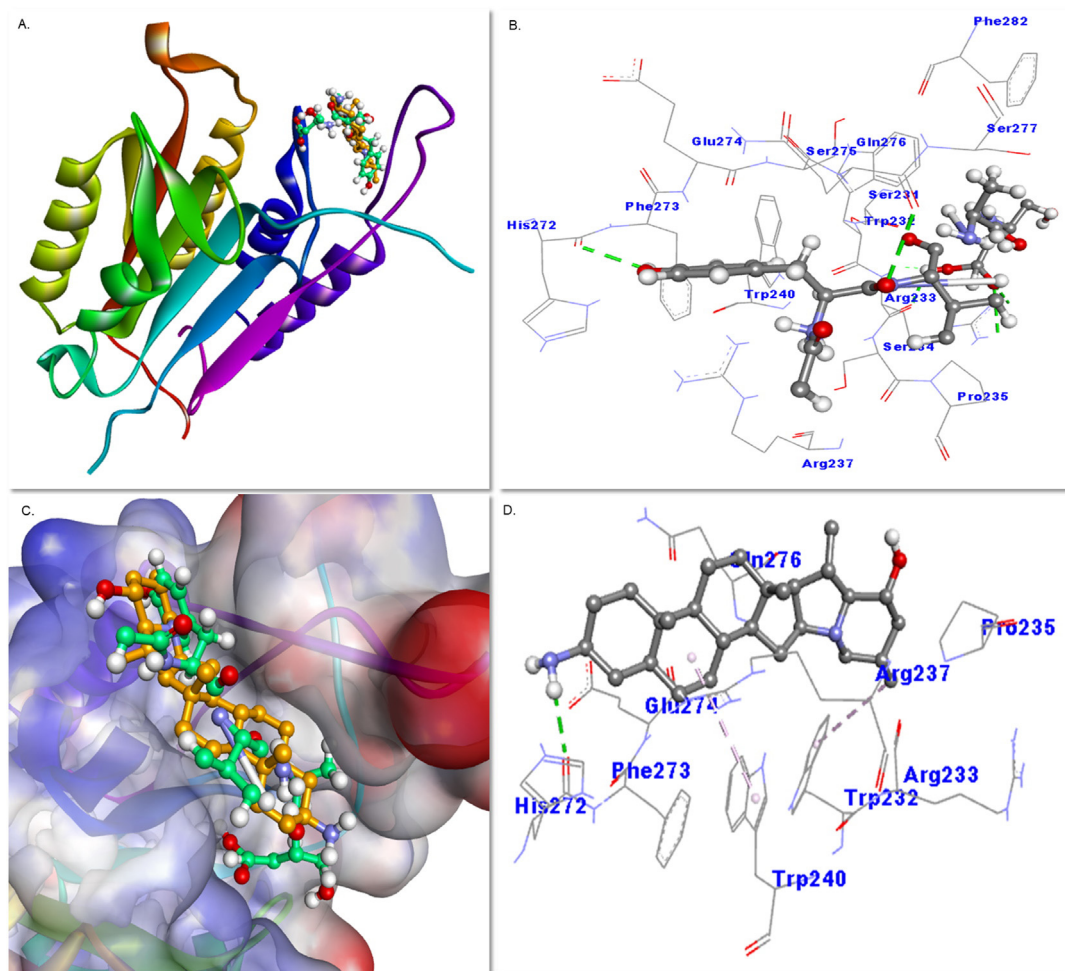


**Fig. 9.** Molecular docking analysis showing structure-based interaction of *S. schimperianum* derived solanopubamine with (A) caspase-7 and (B) Acetyl-YVAD-CHO, the ligand control.

HepG2.2.15 is widely used to test *in vitro* efficacies of anti-HBV molecules. We therefore, assessed the anti-HBV efficacy of solanopubamine in HepG2.2.15 cells. Solanopubamine showed marked anti-HBV activity in a time and dose-dependent manner. At day 5 post-treatment, the 30  $\mu\text{M}$  dose efficiently inhibited HBsAg expression by 66.5%, whereas it markedly down regulated HBeAg synthesis by 70.5%. This could be compared to the reference drug lamivudine (2  $\mu\text{M}$ ) that inhibited HBsAg and HBeAg by 82.5% and 86.5%, respectively. In line with this, protoberberine dehydrocavidine and dehydroapocavidine from *Corydalis saxicola* have been reported to significantly inhibit HBsAg by 53%–59%, and HBeAg by 41%–43%, respectively in HepG2.2.15 cells (Li et al., 2008). Notably, *Evodia fargesii* derived N,N-dimethyltryptamine N12-oxide ( $\text{IC}_{50}$ : 17.6  $\mu\text{M}$ ) markedly downregulated HBV DNA replication in HepG2.2.15 (Qu et al., 2006). As compared to solanopubamine used at 30  $\mu\text{M}$ , *Rhus succedanea* derived robustaflavone ( $\text{IC}_{50}$ : 250  $\mu\text{M}$ ) and robustaflavone hexaacetate ( $\text{IC}_{50}$ : 730  $\mu\text{M}$ ) has been reported for its marked anti-HBV effect by downregulating HBV replication in HepG2.2.15 cells (Zembower et al., 1998). Moreover, dauricumidine, a chlorinated alkaloid isolated from *Hypserpa nitida* was shown to have significant anti-HBV potential in HepG2.2.15 cells (Cheng et al., 2007). Also, the alkaloid squalamine isolated from marine animals (*Squalus Acanthias* and *Petromyzon marinus*) are reported for its antiviral activities via altering HBV virion morphogenesis (Zaslloff et al., 2011).

HBV-polymerase has been the favored viral enzyme towards developing anti-HBV agents, such as nucleoside analogs like lamivudine. However, lamivudine or other such analogs have been widely associated with emergence of drug-resistant HBV variants due to mutations in the polymerase catalytic domain ‘YMDD  $\rightarrow$  YIDD’ motif, posing an important clinical challenge (Devi and Locarnini, 2013). Fortunately, so far there is no report on natural or herbal product associated HBV drug-resistance *in vitro* or *in vivo*. The *Sophora lopecuraidae* derived alkaloid oxy-matine has been reported to inhibit HBV antigens and DNA replication, attributed to interference with HBV polymerase (Wu and Guo, 2004; Mao et al., 2004; Xu et al., 2010). Notably, cepharanthine isolated from *Stephania cepharantha* is shown to inhibit HBeAg expression and DNA replication in lamivudine-resistant HBV clinical isolates (Zhou et al., 2012). In view of this, we modelled both lamivudine-sensitive (wild type: YMDD) and lamivudine-resistant (mutant: YIDD) 3D structures of HBV polymerase, and performed molecular docking with solanopubamine. Interestingly, while lamivudine interacted with the wild-type polymerase ‘YMDD’ motif and formed stable complex, solanopubamine interacted with both ‘YMDD’ as well as ‘YIDD’ motifs and formed stable complexes. Notably, while Tyr203 of ‘YMDD’ was commonly involved in the interaction of wild-type polymerase with lamivudine and solanopubamine, both Trp203 and Asp206 of ‘YIDD’ participated in mutant polymerase interaction with

solanopubamine. Our structure-based virtual analysis therefore, strongly predicts the effectiveness of solanopubamine against lamivudine-resistant HBV mutants.

In experimental setting, DCFH is commonly used to assess *in vitro* oxidative stress and cell death triggered by generation of free radicals due to H<sub>2</sub>O<sub>2</sub> dependent reactions with cytochrome c and Fe<sup>2+</sup> (LeBel et al., 1992; Royall and Ischiropoulos, 1993; Arbab et al., 2015; Arbab et al., 2016; Parvez et al., 2018a, 2018b; Parvez et al., 2019c). Notably, S. surattense previously reported for a steroidal alkaloid solanoside (Lu et al., 2011; Nawaz et al., 2014), has shown strong anti-oxidative and anti-hepatotoxic salutations in HepG2 cells against DCFH-toxicity as well as in CCl<sub>4</sub>-treated rats (Parvez et al., 2019c). In the present study, we therefore, used DCFH to trigger hepatocytotoxicity in cultured HepG2 cells. Cellular cysteine-aspartate proteases such as caspases-3 and caspase-7 play important roles in maintaining cytoplasmic homeostasis through apoptotic and inflammatory activities (Kumar, 2006). Solanopubamine co-treatment attenuated DCFH-induced oxidative and apoptotic damage and restored HepG2 cell viability by 28.5%, and downregulated caspase-3/7 activations by 33%. Further structure-based docking analysis showed that solanopubamine as well the control ligands interacted with some common residues of the substrate-binding and catalytic site of both caspase-3 and caspase-7, and formed stable ligand–protein complexes.

## 5. Conclusion

Our data demonstrates the potential therapeutic efficacies of *S. schimperianum* derived solanopubamine against HBV, which is suggested via interfering with both wild type and drug-resistant mutant polymerase. In addition, solanopubamine also protects liver cells against chemical cytotoxicity through attenuation of free-radicals and downregulation of cellular caspases. This warrants further *in vivo* molecular and pharmacological assessment of solanopubamine.

## Declaration of Competing Interest

The authors declare that they have no known competing financial interests or personal relationships that could have appeared to influence the work reported in this paper.

## Acknowledgement

The authors gratefully acknowledge the Researchers Supporting Project number (RSP-2021/379), King Saud University, Riyadh, Saudi Arabia for funding this work.

## Appendix A. Supplementary data

Supplementary data to this article can be found online at <https://doi.org/10.1016/j.jsps.2022.02.001>.

## References

Agniswamy, J., Fang, B., Weber, I.T., 2009. Conformational similarity in the activation of caspase-3 and -7 revealed by the unliganded and inhibited structures of caspase-7. *Apoptosis*. 14 (10), 1135–1144.

Al-Asmari, A.K., Al-Elaiwi, A., Athar, M.T., et al., 2014. A review of Hepatoprotective plants used in Saudi traditional medicine. *Evid-Based Compl. Alt. Med.* 890842, 890842.

Al-Oqail, M.M., Hassan, W.H.B., Ahmad, M.S., Al-Rehaily, A.J., 2012. Phytochemical and biological studies of *Solanum schimperianum* Hochst. *Saudi Pharm. J.* 20, 371–379.

Al-Rehaily, A.J., Ahmad, M.S., Mustafa, J., Al-Oqail, M.M., Hassan, W.H., Khan, S.I., Khan, I.A., 2013. Solanopubamine, a rare steroidal alkaloid from *Solanum*

*schimperianum*: Synthesis of some new alkyl and acyl derivatives, their anticancer and antimicrobial evaluation. *J. Saudi Chem. Soc.* 17 (1), 67–76.

Al-Shabib, N.A., Khan, J.M., Malik, A., Rehman, M.T., AlAjmi, M.F., Husain, F.M., Ahmad, A., Sen, P., 2020. Investigating the effect of food additive azo dye “tartrazine” on BLG fibrillation under in-vitro condition. A biophysical and molecular docking study. *J. King Saud Univ.– Sci.* 32, 2034–2040.

Angenot, L., 1969. Spectrophotometric and chromatographic study of flavones and coumarin derivatives of *Solanum schimperianum*. *Plants Med. Phytother.* 3, 243–254.

Arbab, A.H., Parvez, M.K., Al-Dosari, M.S., Al-Rehaily, A.J., Ibrahim, K.E., Alam, P., AlSaid, M.S., Rafatullah, S., 2016. Therapeutic efficacy of ethanolic extract of *Aerva javanica* aerial parts in the amelioration of CCl<sub>4</sub>-induced hepatotoxicity and oxidative damage in rats. *Food Nutr. Res.* 60, 30864.

Arbab, A.H., Parvez, M.K., Al-Dosari, M.S., Al-Rehaily, A.J., Al-Sohaibani, M., Zaroug, E.E., AlSaid, M.S., Rafatullah, S., 2015. Hepatoprotective and antiviral efficacy of *Acacia mellifera* leaves fractions against hepatitis B virus. *BioMed Res. Intl.* 2015, 1–10.

Arbab, A.H., Parvez, M.K., Al-Dosari, M.S., Al-Rehaily, A.J., 2017. In vitro evaluation of novel antiviral activities of 60 medicinal plants extract against hepatitis B virus. *Exp. Ther. Med.* 14, 626–634.

Camacho, C., Coulouris, G., Avagyan, V., Ma, N., Papadopoulos, J., Bealer, K., Madden, T.L., 2009. BLAST+: architecture and applications. *BMC Bioinform.* 10, 421–430.

Chaudhary, S.A., 2001. Ministry of Agriculture and Water; Kingdom of Saudi Arabia: Flora of the Kingdom of Saudi Arabia) vol. 2(II).

Cheng, P.i., Ma, Y.-B., Yao, S.-Y., Zhang, Q., Wang, E.-J., Yan, M.-H., Zhang, X.-M., Zhang, F.-X., Chen, J.-J., 2007. Two new alkaloids and active anti-hepatitis B virus constituents from *Hypserpa nitida*. *Bioorg. Med. Chem. Lett.* 19, 5316–5320.

Coune, C., Denoel, A., 1975. Chromatographic study of *Solanum schimperianum* glucoalkaloids. *Plants Med. Phytother.* 19, 14–20.

Devi, U., Locarnini, S., 2013. Hepatitis B antivirals and resistance. *Curr. Opin. Virol.* 3, 495–500.

Ganesan, R., Jelakovic, S., Mittl, P.R.E., Cafilisch, A., Grutter, M.G., 2011. In silico identification and crystal structure validation of caspase-3 inhibitors without a P1 aspartic acid moiety. *Acta Cryst.* F67, 842–850.

Kumar, S., 2006. Caspase function in programmed cell death. *Cell Death Differen.* 14 (1), 32–43.

Kumari, G.N.K., Rao, L.J.M., Rao, N.S.P., Kaneko, K., Mitsushashi, H., 1985. Solanopubamine, a steroidal alkaloid from *Solanum pubescens*. *Phytochemistry*. 24, 369–1371.

Kumari, G.N.K., Rao, L.J.M., Rao, N.S.P., Kaneko, K., Mitsushashi, H., 1986. Solanopubamides A and B, two further steroidal alkaloids from *Solanum pubescens*. *Phytochemistry*. 25, 2003–2004.

LeBel, C.P., Ischiropoulos, H., Bondy, S.C., 1992. Evaluation of the probe 2',7'-dichlorofluorescein as an indicator of reactive oxygen species formation and oxidative stress. *Chem. Res. Toxicol.* 5 (2), 227–231.

Li, H.-L., Han, T., Liu, R.-H., Zhang, C., Chen, H.-S., Zhang, W.-D., 2008. Alkaloids from *Corydalis saxicola* and their anti-hepatitis B virus activity. *Chem. Biodiver.* 5, 777–783.

Lu, Y.Y., Luo, J., Kong, L.Y., 2011. Steroidal alkaloid saponins and steroidal saponins from *Solanum surattense*. *Phytochemistry*. 72, 668–673.

Mao, Y.-M., Zeng, M.-D., Lu, L.-G., Wan, M.-B., Li, C.-Z., Chen, C.-W., Fu, Q.-C., 2004. Capsule oxytetracycline in treatment of hepatic fibrosis due to chronic viral hepatitis: a randomized, double blind, placebo-controlled, multicenter clinical study. *World J. Gastroenterol.* 10, 3269.

Morris, G.M., Huey, R., Lindstrom, W., Sanner, M.F., Bewle, R.K., Goodsell, D.S., Olson, A.J., 2009. Autodock4 and AutoDockTools4: automated docking with selective receptor flexibility. *J. Comput. Chem.* 16, 2785–2791.

Nawaz, H., Ahmed, E., Sharif, A., et al., 2014. Two new steroidal glycosides from *Solanum surattense*. *Chem. Nat. Compd.* 49, 1091–1094.

Parvez, M.K., Ahmed, S., Al-Dosari, M.S., Abdelwahid, M.A.S., Arbab, A.H., Al-Rehaily, A.J., Al-Oqail, M.M., 2021. The novel anti-hepatitis B virus activity of Euphorbia schimperii and its quercetin and kaempferol derivatives. *ACS Omega* 6 (43), 29100–29110. <https://doi.org/10.1021/acsomega.1c04320>.

Parvez, M.K., Al-Dosari, M.S., Arbab, A.H., Al-Rehaily, A.J., Abdelwahid, M.A.S., 2020. Bioassay-guided isolation of anti-hepatitis B virus flavonoid myricetin-3-O-rhamnoside along with quercetin from *Guiera senegalensis* leaves. *Saudi Pharm. J.* 28 (5), 550–559.

Parvez, M.K., Arab, A.H., Al-Dosari, M.S., Al-Rehaily, A.J., 2016. Antiviral natural products against chronic hepatitis B: recent developments. *Curr. Pharm. Des.* 3, 286–293.

Parvez, M.K., Arbab, A.H., Al-Dosari, M.S., Al-Rehaily, A.J., Alam, P., Ibrahim, K.E., AlSaid, M.S., Rafatullah, S., 2018a. Protective effect of *Atriplex suberecta* extract against oxidative and apoptotic hepatotoxicity. *Exp. Ther. Med.* 15, 3883–3891.

Parvez, M.K., Rehman, M.T., Alam, P., Al-Dosari, M.S., Alqasoumi, S.I., Alajmi, M.F., 2019a. Plant-derived antiviral drugs as novel hepatitis B virus inhibitors: cell culture and molecular docking study. *Saudi Pharmaceut. J.* 27, 89–400.

Parvez, M.K., Al-Dosari, M.S., Alam, P., Rehman, M.T., Alajmi, M.F., 2019b. The anti-hepatitis B virus therapeutic potential of anthraquinones derived from *Aloe vera*. *Phytother. Res.* 33, 1960–1970.

Parvez, M.K., Al-Dosari, M.S., Arbab, A.H., Alam, P., AlSaid, M.S., Khan, A.A., 2019c. Hepatoprotective efficacy of *Solanum surattense* extract against chemical-induced oxidative and apoptotic injury in rats. *BMC Compl. Alter Med.* 19, 154–162.

Parvez, M.K., Sehgal, D., Sarin, S.K., Basir, F.B., Jameel, S., 2006. Inhibition of hepatitis B virus DNA replication intermediate forms by recombinant IFN-. *World J. Gastroenterol.* 12, 3006–3014.

- Parvez, M.K., Alam, P., Arbab, A.H., Al-Dosari, M.S., Alhowiriny, T.A., Alqasoumi, S.I., 2018b. Analysis of antioxidative and antiviral biomarkers  $\beta$ -amyrin,  $\beta$ -sitosterol, lupeol, ursolic acid in *Guiera senegalensis* leaves extract by validated HPTLC methods. *Saudi Pharm. J.* 26 (5), 685–693.
- Qu, S.-J., Liu, Q.-W., 2006. New Indole N -Oxide Alkaloids from *Evodia fargesii*. *Planta Med.* 72, 264–266.
- Rahman, M.A., Mossa, J.S., AlSaid, M.S., Al-Yahya, M.A., 2014. Medicinal plant diversity in the flora of Saudi Arabia: a report on seven plant families. *Fitoterapia.* 75, 149–161.
- Rehman, M.T., Ahmed, S., Khan, A.U., 2016. Interaction of Meropenem with 'N' and 'B' isoforms of Human Serum Albumin: a Spectroscopic and Molecular Docking Study. *J. Biomol. Struct. Dyn.* 34, 1849–1864.
- Royall, J.A., Ischiropoulos, H., 1993. Evaluation of 2',7'-dichlorofluorescein and dihydro-rhodamine 123 as fluorescent probes for intracellular H<sub>2</sub>O<sub>2</sub> in cultured endothelial cells. *Arch. Biochem. Biophys.* 302, 348–355.
- Siddiqui, N.A., Parvez, M.K., Al-Rehaily, A.J., Al Dosari, M.S., Alam, P., Shakeel, F., Al Harbi, H.A., 2017. High-performance thin layer chromatography based assay and stress study of a rare steroidal alkaloid solanopubamine in six species of *Solanum* grown in Saudi Arabia. *Saudi Pharm. J.* 25 (2), 184–195.
- Steinegger, M., Meier, M., Mirdita, M., Vöhringer, H., Haunsberger, S.J., Söding, J., 2019. HH-suite3 for fast remote homology detection and deep protein annotation. *BMC Bioinform.* 20, 473.
- Studer, G., Tauriello, G., Bienert, S., Biasini, M., Johner, N., Schwede, T., 2021. ProMod3- A versatile homology modelling toolbox. *PLOS Comp. Biol.* 17, e1008667.
- Tang, L.S.Y., Cover, E., Wilson, E., Kottitil, S., 2018. Chronic hepatitis B infection: a review. *J. Am. Med. Assoc.* 319, 1802–1813.
- Wang, G., Zhang, L., Bonkovsky, H.L., 2012. Chinese medicine for treatment of chronic hepatitis B. *Chin. J. Integr. Med.* 18, 53–55.
- Williams, R., 2006. Global challenges in liver disease. *Hepatology.* 44, 521–526.
- Wu, X.N., Guo, J.W., 2004. Experimental studies of oxymatrine and its mechanisms of action in hepatitis B and C viral infections. *Chinese J Digest. Dis.* 1, 12–16.
- Xu, Wen-S., Zhao, Ke-K., Miao, Xiao-H., Xiong, W.N. Zhang, Rui-Q., Wang, Jun-X., 2010. Effect of oxymatrine on the replication cycle of hepatitis B virus in vitro. *World J. Gastroenterol.* 16, 2028.
- Zasloff, M., Adams, P., Beckerman, B., Campbell, A., Han, Z., Luijten, E., Meza, I., 2011. Squalamine as a broad-spectrum systemic antiviral agent with therapeutic potential. *Proc. Natl. Acad. Sci. USA* 108, 15978–15983.
- Zembower, D.E., Lin, Y.-M., Flavin, M.T., Chen, F.-C., Korba, B., 1998. Robustaflavone, a potential non-nucleoside anti-hepatitis B agent. *Antiviral Res.* 39, 81–88.
- Zhou, Y.-B., Wang, Y.-F., Zhang, Y., Zheng, L.-Y., Yang, X.-A., Wang, N., Jiang, J.-H., 2012. In vitro activity of cepharanthine hydrochloride against clinical wild-type and lamivudine-resistant hepatitis B virus isolates. *European J. Pharmacol.* 683, 10–15.